

The PYRIN domain–only protein POP3 inhibits ALR inflammasomes and regulates responses to infection with DNA viruses

Sonal Khare¹, Rojo A Ratsimandresy¹, Lúcia de Almeida¹, Carla M Cuda¹, Stephanie L Rellick^{2,8}, Alexander V Misharin¹, Melissa C Wallin¹, Anu Gangopadhyay¹, Eleonora Forte³, Eva Gottwein³, Harris Perlman¹, John C Reed^{4,5}, David R Greaves⁶, Andrea Dorfleutner¹ & Christian Stehlik^{1,7}

The innate immune system responds to infection and tissue damage by activating cytosolic sensory complexes called ‘inflammasomes’. Cytosolic DNA is sensed by AIM2-like receptors (ALRs) during bacterial and viral infections and in autoimmune diseases. Subsequently, recruitment of the inflammasome adaptor ASC links ALRs to the activation of caspase-1. A controlled immune response is crucial for maintaining homeostasis, but the regulation of ALR inflammasomes is poorly understood. Here we identified the PYRIN domain (PYD)-only protein POP3, which competes with ASC for recruitment to ALRs, as an inhibitor of DNA virus–induced activation of ALR inflammasomes *in vivo*. Data obtained with a mouse model with macrophage-specific POP3 expression emphasize the importance of the regulation of ALR inflammasomes in monocytes and macrophages.

Germline-encoded pattern-recognition receptors (PRRs) of the innate immune system are essential for host defense against pathogens through the production of proinflammatory mediators and antimicrobial factors. Cytosolic PRRs of the ALR (PYHIN or HIN-200) family and NLR family are necessary for the maturation and release of the proinflammatory cytokines interleukin 1 β (IL-1 β) and IL-18 and the induction of pyroptotic cell death, which requires activation of proinflammatory caspase-1, caspase-4 and caspase-5 (or caspase-1 and caspase-11 in mice) in inflammasomes¹. The inflammasome adaptor ASC bridges PRRs to caspase-1; this facilitates the activation of caspase-1 by induced proximity^{2,3}. In response to viral infection, inflammasomes sense pathogen-associated molecular patterns, including double-stranded RNA, uncapped single-stranded RNA and double-stranded DNA. Thus, unique PRRs exist that sense cytosolic DNA and RNA⁴. In particular, ALRs sense viral DNA and assemble an inflammasome. Whereas AIM2 senses bacterial and viral cytosolic DNA^{5–7}, the interferon-inducible sensor IFI16 detects modified nuclear viral DNA and assembles an initially nuclear inflammasome⁸. ALRs directly bind DNA via their HIN-200 domain^{9,10} and recruit ASC through their PYRIN domain (PYD)^{11–14}. ALRs are diverse in mice versus humans; while only four such proteins exist in humans, mice have thirteen predicted members of this family, but their function is largely unknown^{15,16}.

The antiviral host response depends on the production of interferons. Production of the type II interferon IFN- γ by natural killer (NK) cells depends on IL-18 production in an AIM2 inflammasome-dependent manner⁶, but ALRs also regulate the type I interferon response⁴. Although the activation of inflammasomes is essential for host defense and the clearance of intracellular bacteria, viruses, fungi and parasites, excessive and uncontrolled activation of inflammasomes causes autoinflammatory diseases, and impaired activation promotes metabolic disease. The recognition of self nucleic acids by PRRs directly contributes to the pathology associated with various autoimmune diseases, which emphasizes the importance of balanced regulation of inflammasomes⁴.

The PYD-only proteins (POPs) represent a family of inflammasome regulators, which bind and occupy the PYD in ASC and PYD-containing PRRs and thereby abolish the PYD-PYD interactions necessary for inflammasome formation^{17–19}. Although several species, including humans, mice lack this family of proteins, which suggests the development of a more complex mechanism of inflammasome regulation in some organisms²⁰. However, members of the POP family have not yet been studied *in vivo*. POP1 (PYDC1) is similar to the PYD of ASC and interacts with ASC, thereby affecting the activation of inflammasomes and of the transcription factor NF- κ B¹⁹. POP2 (PYDC2) interacts with the PYD of ASC, as well as with the PYDs of

¹Division of Rheumatology, Department of Medicine, Feinberg School of Medicine, Northwestern University, Chicago, Illinois, USA. ²Program in Cancer Cell Biology, Health Sciences Center, West Virginia University, Morgantown, West Virginia, USA. ³Department of Microbiology and Immunology, Feinberg School of Medicine, Northwestern University, Chicago, Illinois, USA. ⁴Apoptosis and Cell Death Research Program, Sanford-Burnham Medical Research Institute, La Jolla, California, USA. ⁵Pharma Research and Early Development, F. Hoffmann–La Roche, Basel, Switzerland. ⁶Sir William Dunn School of Pathology, University of Oxford, Oxford, UK. ⁷Robert H. Lurie Comprehensive Cancer Center, Interdepartmental Immunobiology Center and Skin Disease Research Center, Feinberg School of Medicine, Northwestern University, Chicago, Illinois, USA. ⁸Present address: Center for Neuroscience, Health Sciences Center, West Virginia University, Morgantown, West Virginia, USA. Correspondence should be addressed to C.S. (c-stehlik@northwestern.edu) or A.D. (a-dorfleutner@northwestern.edu).

Received 19 November 2013; accepted 14 January 2014; published online 16 February 2014; doi:10.1038/ni.2829

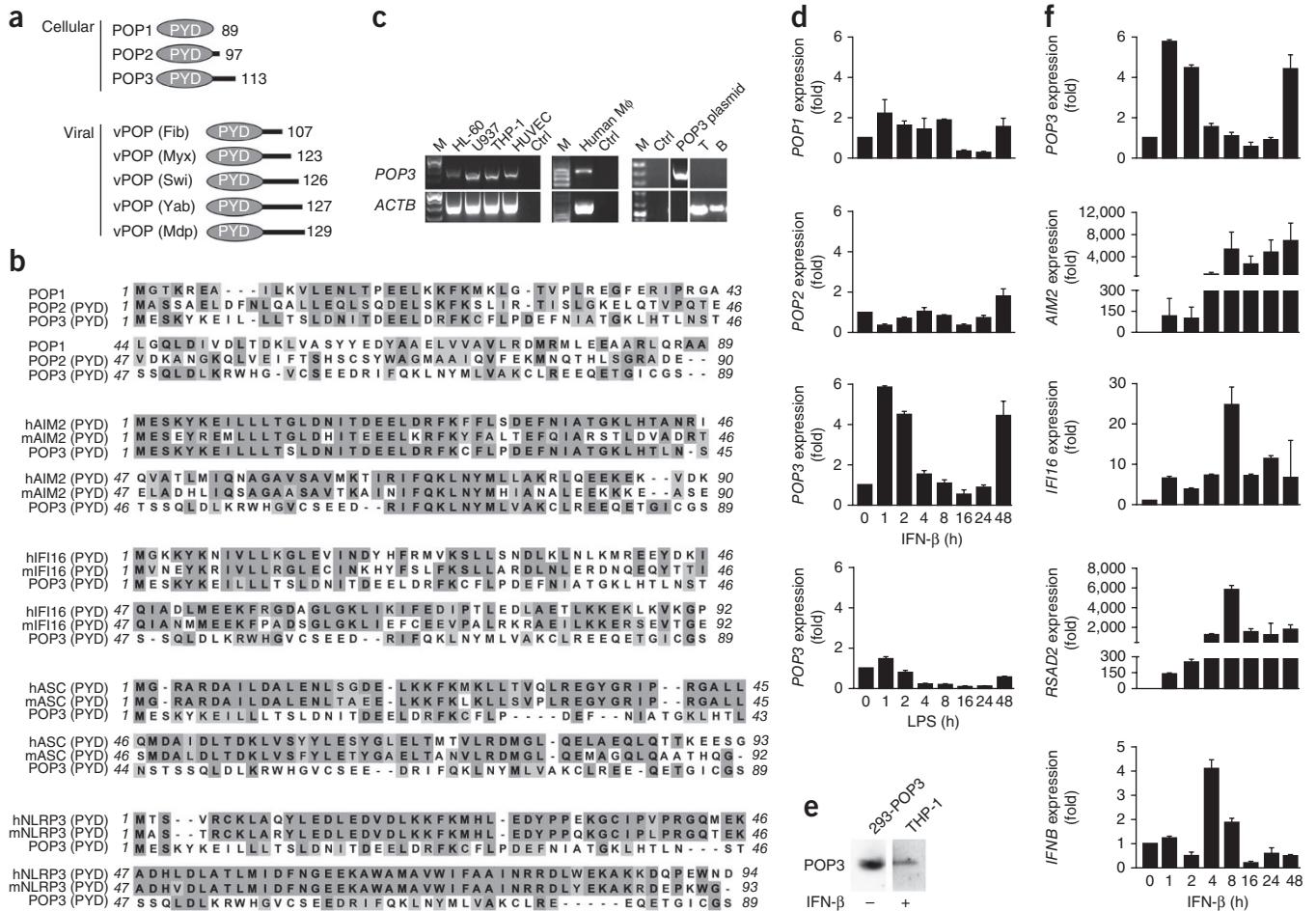


Figure 1 POP3 is a previously unknown type I interferon-inducible member of the POP family. **(a)** Cellular and viral members of the POP family; right margin, size (in amino acids). Fib, Shope fibroma virus; Myx, myxoma virus; Swi, swinepox virus; Yab, Yaba-like disease virus; Mdp, mule deer poxvirus. **(b)** Sequence alignment for members of the human POP family and POP3 and the PYDs of human (h) and mouse (m) AIM2, IFI16, ASC and NLRP3. **(c)** RT-PCR analysis of *POP3* expression in HL-60 human promyelocytic leukemia cells, U937 human leukemic monocyte lymphoma cells, THP-1 cells, human umbilical vein endothelial cells (HUVEC), a negative, no-template control without cells (Ctrl), and human macrophages (M Φ), T cells (T) and B cells (B), as well as RT-PCR analysis of a *POP3* plasmid; *ACTB* (encoding β -actin) serves as a loading control. M, molecular size markers. **(d)** Real-time PCR analysis of *POP1*, *POP2* and *POP3* in human primary macrophages treated for 0–48 h with LPS or IFN- β (horizontal axes); results are presented relative to those of untreated cells (0), set as 1. **(e)** Immunoblot analysis of POP3 in THP-1 cells treated for 48 h with IFN- β and in control HEK293 cells transfected with POP3-encoding cDNA (293-POP3). **(f)** Real-time PCR analysis of *POP3*, *AIM2*, *IFI16*, *RSAD2* and *IFNB* in human primary macrophages treated for 1–48 h (horizontal axes) with IFN- β (presented as in **d**). Data are representative of two experiments (error bars (**d**,**f**), s.e.m. of three replicates).

several members of the PYD-containing NLR family¹⁸. POP2 also prevents NLR-mediated activation of NF- κ B²¹. The importance of POPs in regulating host defense is emphasized by the finding that certain poxviruses express a viral POP to evade the host immune response by blocking the activation of inflammasomes and NF- κ B^{17,22}.

Here we report the discovery of a previously undescribed type I interferon-inducible member of the POP family, POP3, which interacted with the ALRs AIM2 and IFI16 to inhibit the formation of ALR inflammasomes. Thus, we have obtained evidence that each main branch of inflammasome-activating PRRs evolved a POP regulator in humans. Silencing of POP3 in human macrophages enhanced DNA- and DNA virus-induced formation of ALR inflammasomes and hence the maturation and release of IL-1 β and IL-18. Consistent with that, expression of POP3 (which is not naturally expressed by mice) specifically in cells of the monocyte-macrophage lineage in transgenic mice impaired an ALR inflammasome response. Thus, POP3 functioned as a key regulator of ALR inflammasomes in human and mouse macrophages and *in vivo* in a mouse model of viral infection. This also

represents the first macrophage-specific mouse model for the study of inflammasomes, to our knowledge, and our data emphasize that inhibition of ALRs in macrophages was sufficient to impair systemic production of IL-18 and subsequent production of IFN- γ to regulate the antiviral host response, which recapitulates global deficiency in AIM2.

RESULTS

Expression of POP3 in response to type I interferons

We identified a previously unknown member of the human POP family, which we called ‘POP3’ (GenBank/EMBL/DDBJ accession code, [KF562078](#); **Fig. 1a**). Analysis of cDNA encoding POP3 revealed an open reading frame of 342 base pairs (**Supplementary Fig. 1a**) in a single exon located in the interferon-inducible gene cluster between *IFI16* (which encodes IFI16) and *PYHIN1* (which encodes the PYD- and HIN domain-containing protein PYHIN1) on chromosome 1q23, which also encodes the PYHIN family members AIM2 and MND1A (‘myeloid cell nuclear differentiation antigen’) (**Supplementary Fig. 1b**).

Table 1 Sequence identity of POP3 and human and mouse proteins

	hAIM2	mAIM2	hIFI16	mIFI16	hASC	mASC	hNLRP3	mNLRP3	POP1	POP2
POP3 identity (%)	60.9	43.5	17.4	15.2	18.9	16.8	20.2	12.5	21.7	11.1

Sequence identity of POP3 and various human and mouse proteins (those aligned in Fig. 1b), assessed with the BLOSUM substitution matrix.

In comparison, the syntenic mouse chromosomal region 1H3 is amplified and contains 13 predicted genes but does not encode an ortholog of POP3 (refs. 15,16). POP3 encoded a single PYD of 113 amino acids with five predicted α -helices (Supplementary Fig. 2a), whereas the PYD of AIM2 consists of six α -helices. Hence, the third α -helix of the PYD of AIM2 seemed to be unstructured in POP3 (Supplementary Fig. 2a), reminiscent of the structure of the PYD of NLRP1, which forms a flexible loop instead of a third α -helix and is predicted to become stabilized upon PYD-PYD interactions²³. POP1, POP2 and POP3 exhibited low sequence homology to each other (Fig. 1b), which indicated that they might have unique functions. In contrast to POP1 and POP2, POP3 showed high sequence similarity to the PYD of AIM2 (Fig. 1b and Table 1) and showed overall high similarity to the PYDs of members of the HIN-200 family²⁴ (Supplementary Fig. 2b). POP3 shared several of the characteristic sequence motifs in the first and second α -helices of HIN-200 PYDs, but not those in the fifth and sixth α -helices (Supplementary Fig. 2c). Phylogenetic-tree analysis of all PYD-containing proteins also placed POP3 in the HIN-200 family (Supplementary Fig. 2d). Thus, POP3 most probably originated from duplication of the exon encoding the PYD of AIM2; this is reminiscent of POP1, which is derived from the PYD of ASC¹⁹. Consistent with that, POP3 had low sequence homology with the PYDs of mouse and human ASC and the cytoplasmic receptor NLRP3 (Fig. 1b and Table 1). POP3 mRNA was expressed in human monocytic cell lines and human primary macrophages but not in human B cells or T cells (Fig. 1c). Similar to ALR expression, POP3 expression was upregulated in response to IFN- β in human primary macrophages, but lipopolysaccharide (LPS), the agonist of Toll-like receptor 4 (TLR4), did not induce POP3 expression (Fig. 1d). Accordingly, we also detected POP3 by immunoblot analysis of IFN- β -treated THP-1 human macrophages (Fig. 1e). The POP3 expression pattern was unique, since neither PYDC1 (which encodes POP1; called 'POP1' here) nor PYDC2 (which encodes POP2; called 'POP2' here) was regulated by IFN- β (Fig. 1d), which emphasized a selective role for POP3 in the type I interferon-mediated host response. POP3 expression was upregulated as an early response within the first 2 h of IFN- β treatment, as well as a late response after 48 h, distinct from the expression patterns of AIM2, IFI16, IFNB1 and the interferon-stimulated gene RSAD2 (also known as VIPERIN) (Fig. 1f). Thus, the IFN- β -inducible protein POP3 was a member of the POP family and showed similarity to the PYDs of HIN-200 proteins.

POP3 binds to ALRs and inhibits inflammasome formation

Since PYDs usually exhibit homotypic interactions and POP3 contained several HIN-200 PYD-specific sequence motifs and displayed high homology to the PYD of AIM2, we investigated whether POP3 was able to bind to the PYD of HIN-200 proteins. For this we assessed POP3 bound to glutathione S-transferase (GST-POP3). We found that GST-POP3 bound to the PYD of AIM2 and IFI16, but the GST-only control did not (Fig. 2a). However, GST-POP3 showed no substantial interaction with the PYDs of MDA5 or PYHIN1 (Fig. 2a). We confirmed that interaction by coimmunoprecipitation of those proteins from HEK293 human embryonic kidney cells transiently transfected to express POP3 and either AIM2 or IFI16 (Fig. 2b).

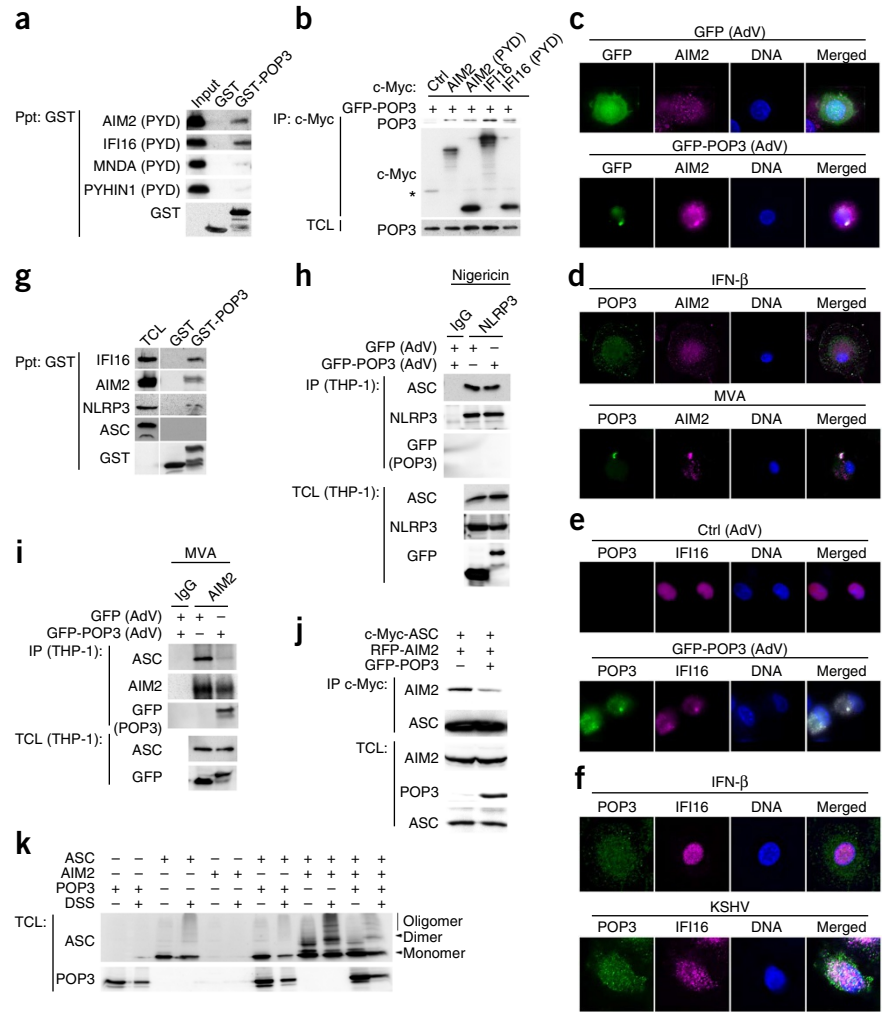
Those observations were further supported by the results of colocalization studies. AIM2 and IFI16 have been shown to localize

together with ASC, albeit at different sites and in response to different stimuli^{8,12,13}. While DNA from modified vaccinia virus Ankara (MVA) and mouse cytomegalovirus (MCMV) is sensed by AIM2 in the cytosol^{11–14}, modified DNA originating from latent infection with Kaposi's sarcoma-associated herpesvirus (KSHV) is recognized by IFI16 in the nucleus *in vitro*⁸. AIM2 was present mainly in cytosolic punctate structures, and this pattern was not altered in response to infection with adenovirus expressing green fluorescent protein (GFP) alone (Fig. 2c), while adenovirus-mediated expression of GFP-tagged POP3 (GFP-POP3) resulted in the colocalization of GFP-POP3 and endogenous AIM2 in cytoplasmic punctate structures (Fig. 2c). We also observed very limited colocalization of endogenous AIM2 with endogenous POP3 in a few cytosolic punctate structures in human primary macrophages treated with IFN- β to upregulate the expression of AIM2 and POP3 (Fig. 2d), but that colocalization was greatly enhanced 2 h after infection with MVA (Fig. 2d). In contrast to the predominantly cytosolic localization of AIM2, IFI16 localizes in the nucleus in endothelial cells, where it interacts with ASC⁸. Similarly, we observed solely nuclear localization of IFI16 in human primary macrophages, which was not altered in response to infection with control adenovirus expressing β -galactosidase (Fig. 2e). However, in response to adenovirus-mediated expression of GFP-POP3, IFI16 was redistributed to the cytosol, where it partially localized together with GFP-POP3 (Fig. 2e). In agreement with those results, we did not observe colocalization of endogenous IFI16 and POP3 in IFN- β -treated human primary macrophages (Fig. 2f), nor did infection with MVA alter the distribution of IFI16 or promote its localization together with POP3 at the times assessed (data not shown). However, infection with KSHV caused partial redistribution of IFI16 to the cytosol as early as 2 h after infection (data not shown), which was more prominent at 8 h after infection. At that time, we observed partial localization of IFI16 together with POP3 (Fig. 2f), although KSHV did not cause aggregation of IFI16 in human primary macrophages at the titer used in our experiments (Fig. 2f). These results further supported the proposal of an interaction of POP3 with ALRs.

In agreement with the results presented above, GST-POP3 also precipitated endogenous AIM2 and IFI16 (Fig. 2g). However, in contrast to POP1 and POP2 (refs. 18,19), POP3 did not bind to ASC (Fig. 2g). Unexpectedly, we also observed weak binding of recombinant POP3 to NLRP3 *in vitro* (Fig. 2g), despite their rather low degree of homology and the presence of HIN-200 PYD-specific sequence motifs in POP3. Assembly of the inflammasome through PYD-PYD interactions is a key step for its activation and subsequent cytokine release. The PYDs of ALRs and NLRP3 are known to interact with the PYD of ASC, and we hypothesized that the PYD-containing protein POP3 could interfere with that interaction. In contrast to the interaction of recombinant POP3 with NLRP3 *in vitro*, POP3 was not recruited to and did not disrupt the NLRP3-ASC complex in LPS-primed and nigericin-treated THP-1 cells (Fig. 2h). However, POP3 was recruited to and disrupted the endogenous AIM2-ASC complex in response to the infection of THP-1 cells with MVA (Fig. 2i). Moreover, POP3 also caused less interaction of ectopically expressed ASC and AIM2 in HEK293 cells, as assessed by coimmunoprecipitation (Fig. 2j); this indicated that POP3 was able to disrupt assembly of the ALR inflammasome complex by competing with ASC for the PYD-binding site

Figure 2 POP3 interacts with ALRs.

(a) Precipitation (Ppt) of GST or GST-POP3 with the PYDs of AIM2, IFI16, MNDA and PYHIN1 transcribed and translated *in vitro*. Input, 5% of cleared lysates. (b) Immunoprecipitation (IP) of proteins from HEK293 cells transfected to express GFP-POP3 and vector alone (Ctrl) or c-Myc-tagged full-length AIM2 or IFI16 or the PYD of AIM2 and IFI16 (above lanes), followed by immunoblot analysis of immunoprecipitates with anti-GFP (top) or anti-c-Myc (middle). Bottom (TCL), immunoblot analysis of total cell lysates with anti-POP3. *, cross-reactive protein. (c–f) Immunofluorescence microscopy of human primary macrophages infected for 36 h with adenovirus (AdV) expressing GFP and β -galactosidase (control; GFP) or GFP-POP3 (c,e) or treated for 16 h with IFN- β (d,f) or infected for 2 h with MVA (d) or for 8 h with KSHV (f), followed by immunostaining for AIM2 (c,d) or IFI16 and POP3 (e,f); nuclei are stained with the DNA-intercalating dye DAPI. (g) Precipitation of GST alone (negative control) or GST-POP3 together with endogenous proteins from IFN- β -treated THP-1 cells, and immunoblot analysis of total cell lysates of those cells without precipitation (TCL). (h,i) Immunoprecipitation of proteins, with antibody to NLRP3 (h) or AIM2 (i) or with control immunoglobulin G (IgG; h,i), from THP-1 cells infected with adenovirus expressing GFP or GFP-POP3 or both, then primed with LPS and treated with nigericin (h) or infected with MVA (i), followed by immunoblot analysis (alongside total cell lysates without immunoprecipitation). (j) Immunoprecipitation of proteins, with anti-c-Myc, from HEK293 cells transfected to express c-Myc-tagged ASC, red fluorescent protein (RFP)-tagged AIM2 and/or GFP-POP3, followed by immunoblot analysis (alongside total cell lysates). (k) Immunoblot analysis of ASC oligomerization in HEK293 cells transfected to express ASC, AIM2 and/or POP3 (above lanes), followed by crosslinkage of lysates with disuccinimidylyl suberate (DSS +) or no crosslinkage (DSS –). Data are representative of two experiments.



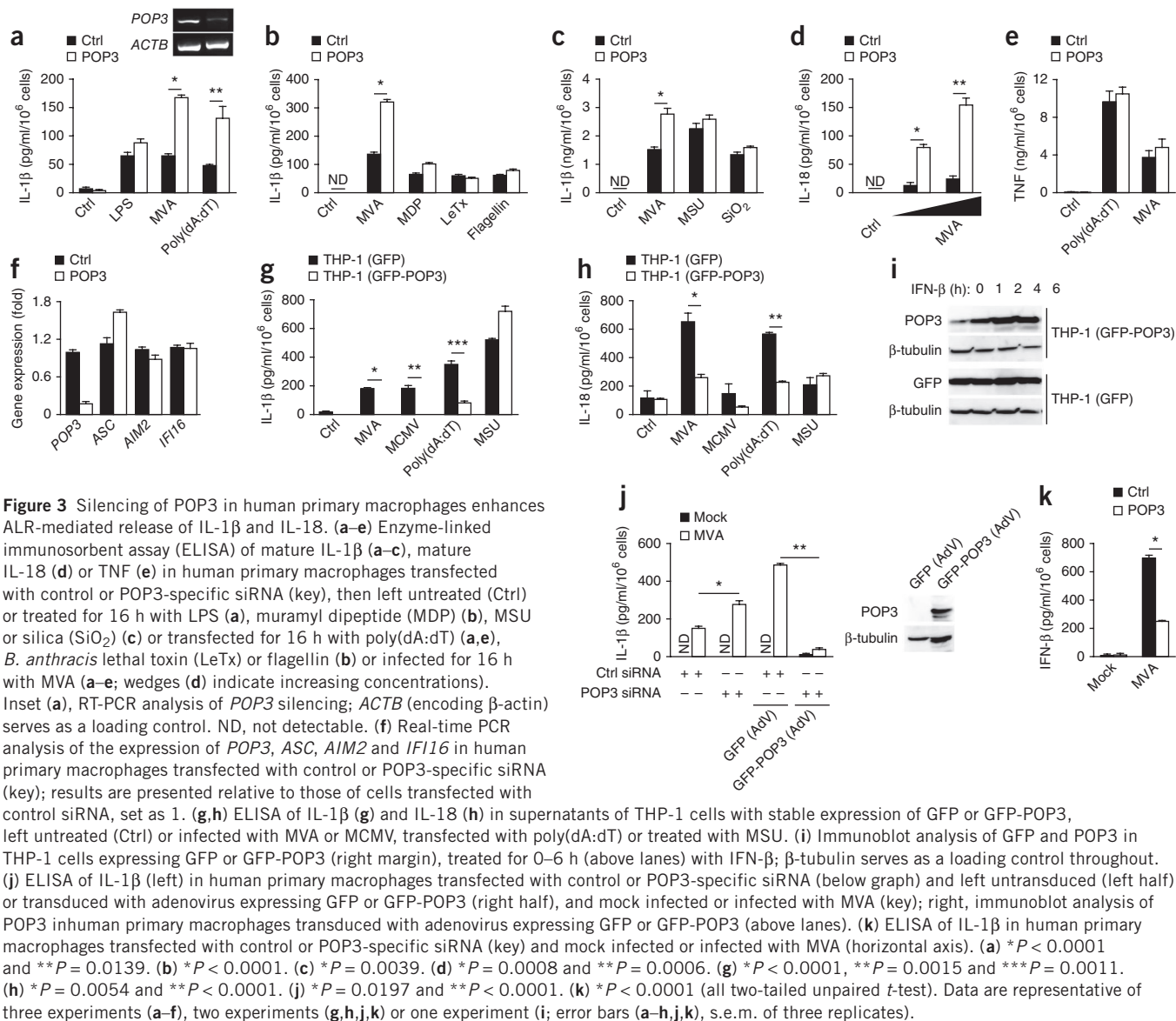
in AIM2. These data suggested that POP3 functioned selectively as an inhibitor of the ALR inflammasome.

Assembly of the AIM2 inflammasome causes the formation of ASC oligomers¹². Transfection of HEK293 cells to express both AIM2 and ASC resulted in the formation of ASC dimers and oligomers, but transfection of those cells to express both ASC and POP3 or to express POP3, ASC or AIM2 alone did not (Fig. 2k). However, in the presence of POP3, the abundance of AIM2-mediated ASC dimers and oligomers was much lower (Fig. 2k), which supported our hypothesis that POP3 was able to inhibit the PYD-dependent recruitment of ASC to AIM2. These data identified POP3 as a previously unknown IFN- β -inducible protein that directly interacted with the ALRs AIM2 and IFI16 through PYD-PYD interactions to prevent inflammasome formation.

POP3 inhibits ALR-mediated release of IL-1 β and IL-18

In response to infection with DNA viruses, AIM2 and IFI16 function as inflammasome-activating DNA-sensors in the cytosol and nucleus, respectively^{5–8}. We silenced the expression of POP3 in human primary macrophages through the use of small interfering RNA (siRNA), as determined by RT-PCR (Fig. 3a), and found that in the absence of POP3, the release of IL-1 β was significantly enhanced in response to

the presence of cytosolic double-stranded DNA, achieved by transfection of poly(dA:dT) or infection with MVA (Fig. 3a). We also obtained similar results with a second POP3-targeting siRNA (Supplementary Fig. 3a). However, silencing of POP3 did not affect the release of IL-1 β triggered by the activation of non-ALR inflammasomes, including inflammasome responses to LPS; the NLRP1 inflammasome response to the lethal toxin of *Bacillus anthracis*²⁵ and muramyl dipeptide²⁶; the NLRP3 inflammasome response to monosodium urate (MSU) crystals²⁷ or silica^{28–30}; or the NLRC4 inflammasome response to *S. typhimurium* flagellin^{31,32} (Fig. 3a–c). THP-1 cells are widely used to study inflammasome responses; after silencing POP3 in THP-1 cells, we observed elevated AIM2-dependent release of IL-1 β in response to AIM2-dependent stimuli but not in response to NLRP3-dependent stimuli (Supplementary Fig. 3b). We also observed increased MVA-induced release of IL-18 after POP3 was silenced in human primary macrophages (Fig. 3d). That effect of POP3 was specific for inflammasome-dependent cytokines, as release of the inflammasome-independent cytokines tumor-necrosis factor (TNF) (Fig. 3e) and IL-6 (Supplementary Fig. 3c) was not affected by silencing of POP3. Silencing of POP3 also did not affect the expression of ASC mRNA, AIM2 mRNA or IFI16 mRNA, as determined by real-time PCR analysis (Fig. 3f), or the respective protein expression (Supplementary Fig. 3d).

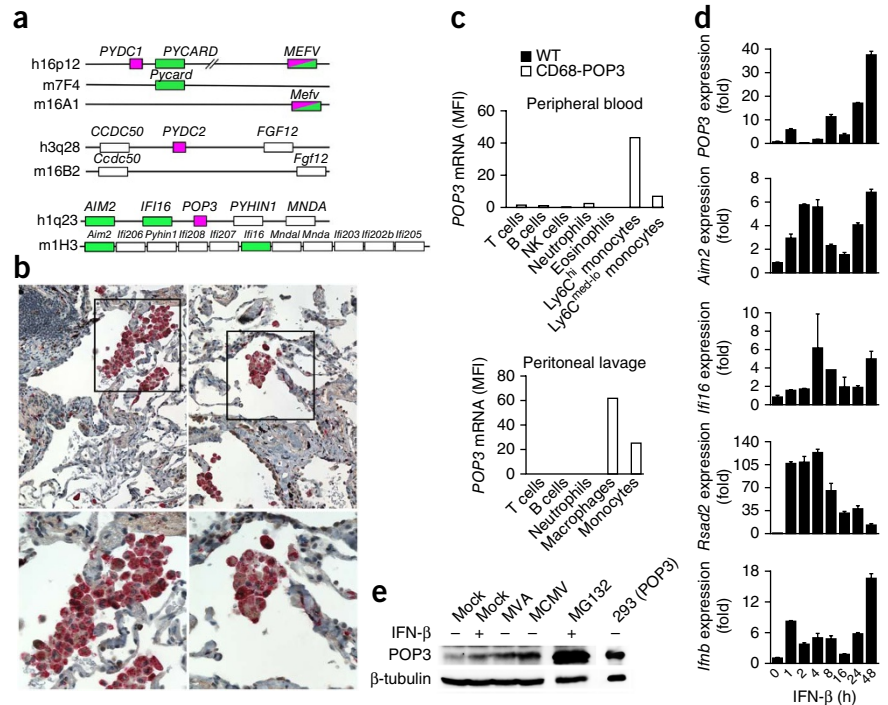


Conversely, THP-1 cells stably expressing GFP-POP3 showed significantly less release of IL-1 β (Fig. 3g) and IL-18 (Fig. 3h), but not of TNF (Supplementary Fig. 3e), in response to infection with MVA or MCMV or transfection of poly(dA:dT), but not in response to MSU crystals, compared with THP-1 cells stably expressing the GFP-only control adenovirus. Those observations further supported the results we obtained with human primary macrophages upon silencing of POP3. Moreover, that cell system also recapitulated the IFN- β -inducible expression of POP3 (Fig. 3i). We next used adenoviral delivery of GFP-POP3 to restore POP3 expression in human primary macrophages in which POP3 was silenced and confirmed the restoration by immunoblot analysis (Fig. 3j). While transduction of GFP-expressing adenovirus into cells transfected with control siRNA slightly enhanced the MVA-induced secretion of IL-1 β , transduction of adenovirus expressing GFP-POP3 strongly suppressed that response (Fig. 3j). Overall our data suggested that POP3 functioned as an inhibitor of DNA-induced activation of inflammasomes but had no effect on NLRP1, NLRP3 or NLRP4 inflammasomes. In addition to having defective inflammasome activation, *Aim2*^{-/-} macrophages show elevated IFN- β

production in response to double-stranded DNA or infection with MVA or bacteria through an as-yet-unknown mechanism^{6,12,13}, and IFI16 functions as a sensor that promotes IFN- β production in response to infection with a DNA virus³³. In agreement with the elevated IFN- β secretion in *Aim2*^{-/-} macrophages, which indicates that AIM2 may negatively regulate IFN- β production, we observed that silencing of *POP3* decreased IFN- β production in human primary macrophages in response to infection with MVA (Fig. 3k), and in THP-1 cells transfected with poly(dA:dT) (Supplementary Fig. 3f). Conversely, THP-1 cells with stable expression of GFP-POP3 displayed elevated IFN- β production in response to AIM2-specific stimuli, but those with stable expression of GFP alone did not (Supplementary Fig. 3g). Further studies are needed to determine whether IFN- β production induced by VACV70, a conserved poxvirus double-stranded DNA sequence motif that is dependent on IFI16 (ref. 33), is also affected by POP3 and the mechanism by which POP3 regulates IFN- β production. Collectively, these results indicated that POP3 functioned as an inhibitor of ALR inflammasome-mediated release of IL-1 β and IL-18 in human macrophages and promoted a type I interferon response.

Figure 4 Monocyte-macrophage lineage-specific expression of POP3 in CD68-POP3 mice.

(a) POP-encoding human chromosomal regions and the syntenic mouse chromosomes: green, sequence encoding inflammasome-activating protein; magenta, sequence encoding POPs. (b) Immunohistochemical staining of CD68 (red) and POP3 (brown) in tissues from inflamed human lungs. Bottom, enlargement of boxed area above. Original magnification, $\times 10$ (top) or $\times 40$ (bottom). (c) POP3 mRNA in populations of peripheral blood cells (top) and peritoneal lavage cells (bottom) isolated 6 h after infection of wild-type (WT) and CD68-POP3 mice with MCMV and identified with specific lineage markers by flow cytometry, presented as mean fluorescence intensity (MFI). (d) Real-time PCR analysis of POP3, *Aim2*, *Ifi16*, *Rsad2* and *Ifnb* in CD68-POP3 BMDMs treated for 0–48 h (horizontal axes) with IFN- β . (e) Immunoblot analysis of POP3 in CD68-POP3 BMDMs treated for 16 h with (+) IFN- β or not (–) and mock infected (Mock) or infected for 16 h with MVA or MCMV, or treated with IFN- β and the proteasome inhibitor MG132 (control), and in HEK293 cells transiently transfected to express POP3 (control). Data are representative of two experiments (b,d,e; error bars (d), s.e.m. of three replicates) or three experiments (c).



Transgenic mice with macrophage-specific POP3 expression

Mice lack POP1 and POP2 (ref. 20). Similar to the close chromosomal locations of the genes encoding POP1 and ASC, the sequence encoding POP3 was next to the genes encoding AIM2 and IFI16, and sequence encoding POP3 was also absent in mice (Fig. 4a), despite substantial amplification of this gene cluster^{15,34}. To study POP3 function *in vivo*, in particular its role in the regulation of inflammasomes in macrophages, we generated mice with transgenic expression of the human POP3 gene from the promoter of the human gene encoding the lysosomal glycoprotein CD68 in combination with the IVS-1 intron, which contains a macrophage-specific enhancer (CD68-POP3 mice)^{35,36}; this seemed the most promising strategy after we tested several commonly used macrophage-specific promoters (data not shown). We further based our promoter choice on our observation that POP3 was specifically expressed in human CD68⁺ macrophages in inflamed lung lesions (Fig. 4b), as assessed with a ‘custom-raised’ antibody that did not cross-react with other POPs or with the related PYDs of IFI16 and AIM2 (Supplementary Fig. 3h,i). Analysis of POP3 mRNA in the CD68-POP3 mice by flow cytometry verified expression specifically in the monocyte-macrophage lineage and particularly in CD11b⁺Ly6C^{hi} classical monocytes in peripheral blood and in CD11b⁺F4/80⁺ peritoneal macrophages (Fig. 4c and Supplementary Fig. 4); this represented the first macrophage-specific mouse model for the study of inflammasomes and the first mouse model for the study of POPs, to our knowledge. The low POP3 expression in bone marrow-derived macrophages (BMDMs) generated from CD68-POP3 mice was induced by IFN- β as an early and late response at the transcriptional level (Fig. 4d), which closely resembled its regulation observed in human primary macrophages. *Aim2*, *Ifi16* and *Rsad2* showed greater inducibility in human primary macrophages (Fig. 1f) than in BMDMs, despite the similar *Ifnb* transcription in these cells (Fig. 4d). Similarly, POP3 protein was inducibly expressed in response to IFN- β or infection with MVA or MCMV (Fig. 4e). We also observed that the expression of POP3 protein was stabilized by the proteasome

inhibitor MG132 (Fig. 4e), which indicated that POP3 expression was tightly regulated not only on the transcriptional level but also on the post-translational level. The proposal of post-translational regulation was further supported by the observation that THP-1 cells expressing GFP-POP3 from the constitutive CMV promoter (instead of the inducible promoter used in mice) had higher expression of POP3 protein after treatment with IFN- β than did their untreated counterparts (Fig. 3i). Overall, these results supported the rationale for using this particular POP3 mouse model.

POP3 inhibits ALR-mediated cytokine release in BMDMs

Next we analyzed the effect of POP3 expression on AIM2 and other inflammasomes. Consistent with the enhanced inflammasome responses we observed in the absence of POP3 in human primary macrophages, POP3 expression resulted in a significantly less release of IL-1 β from CD68-POP3 BMDMs than from wild-type BMDMs in response to transfection of poly(dA:dT) or infection with MVA or MCMV but not in response to muramyl dipeptide, flagellin, LPS plus ATP, or MSU crystals (Fig. 5a,b); we obtained the same results for mouse peritoneal macrophages (Supplementary Fig. 5a). These results emphasized that POP3 had the same selectivity for the AIM2 inflammasomes in mice and humans without affecting NLRP1b, NLRC4 or NLRP3 inflammasomes^{25,27,31,32,37}. As noted above, whereas DNA from MVA and MCMV is sensed by AIM2 in the cytosol, modified DNA originating from latent infection with KSHV is recognized by IFI16 in the nucleus *in vitro*⁸. Given our observation that POP3 and IFI16 were able to interact, we investigated the release of IL-1 β in response to infection with KSHV and found it was significantly lower in CD68-POP3 BMDMs than in wild-type BMDMs (Fig. 5c), which established the proposal that POP3 impaired the AIM2 inflammasome and probably also the IFI16 inflammasome. However, IFI16-dependent sensing of KSHV still must be confirmed *in vivo* by studies of IFI16-deficient mice. As for human primary macrophages, POP3 also inhibited DNA virus-induced release of IL-18 (Fig. 5d)

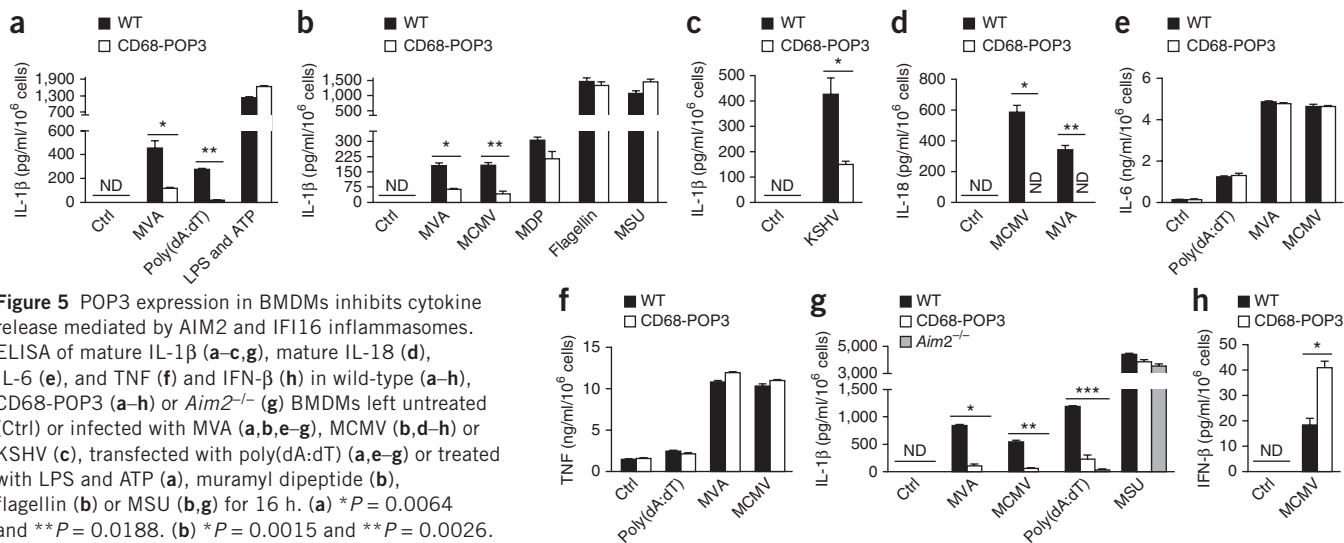


Figure 5 POP3 expression in BMDMs inhibits cytokine release mediated by AIM2 and IFI16 inflammasomes. ELISA of mature IL-1 β (**a–c,g**), mature IL-18 (**d**), IL-6 (**e**), and TNF (**f**) and IFN- β (**h**) in wild-type (**a–h**), CD68-POP3 (**a–h**) or *Aim2*^{-/-} (**g**) BMDMs left untreated (Ctrl) or infected with MVA (**a,b,e–g**), MCMV (**b,d–h**) or KSHV (**c**), transfected with poly(dA:dT) (**a,e–g**) or treated with LPS and ATP, muramyl dipeptide (**b**), flagellin (**b**) or MSU (**b,g**) for 16 h. (**a**) **P* = 0.0064 and ***P* = 0.0188. (**b**) **P* = 0.0015 and ***P* = 0.0026. (**c**) **P* = 0.0020. (**d**) **P* < 0.0001 and ***P* < 0.0001. (**g**) **P* < 0.0001, ***P* = 0.0004 (CD68-POP3) or 0.0009 (*Aim2*^{-/-}) and ****P* = 0.0003 (CD68-POP3) or <0.0001 (*Aim2*^{-/-}). (**h**) **P* = 0.0037 (all two-tailed unpaired *t*-test). Data are representative of three (**a–g**) or two (**c,h**) experiments (error bars, s.e.m. of three (**a,b,d–h**) or six (**c**) replicates).

but did not alter release of the caspase-1-independent inflammatory cytokines IL-6 and TNF from CD68-POP3 BMDMs (**Fig. 5e,f**). To ensure that random transgenic integration of POP3 was not responsible for the phenotype observed, we confirmed our findings with an independent, second transgenic line and obtained identical results (**Supplementary Fig. 5b**). We further generated transgenic mice with ubiquitous expression of the human coxsackie and adenovirus receptor with deletion of the cytoplasmic domain³⁸, driven by the promoter of the gene encoding ubiquitin C³⁹ (**Supplementary Fig. 5c**), which allowed efficient infection with recombinant adenovirus at a low multiplicity of infection (**Supplementary Fig. 5d**). Infection of BMDMs from those mice with adenovirus expressing GFP alone (control) or GFP-POP3 further confirmed that the inhibitory effect of POP3 on the AIM2-induced release of IL-1 β was independent of the site of integration of POP3 (**Supplementary Fig. 5e**). As expected, given the low ectopic expression of an inhibitor such as POP3, the AIM2-mediated release of IL-1 β was not completely abolished in the presence of POP3 but nevertheless reached levels close to those of *Aim2*^{-/-} macrophages in response to AIM2-dependent stimuli (**Fig. 5g**). Neither CD68-POP3 BMDMs nor *Aim2*^{-/-} BMDMs showed diminished release of IL-1 β in response to MSU (**Fig. 5g**). In agreement with our observation that silencing of POP3 in human primary macrophages and THP-1 cells partially inhibited IFN- β production (**Fig. 3k** and **Supplementary Fig. 3f**), POP3-expressing BMDMs produced more IFN- β in response to infection with MCMV than did wild-type BMDMs (**Fig. 5h**), reminiscent of *Aim2*^{-/-} macrophages⁶. Type I interferons block the synthesis of IL-1 α and IL-1 β through an autocrine mechanism dependent on IL-10 and the transcription factor STAT3 (ref. 40) while simultaneously upregulating expression of the IL-1 receptor antagonist IL-1RA and the IL-18 binding protein IL-18BP so they can compete with IL-1 β and IL-18, respectively, for receptor binding^{41,42}. Consistent with that, we observed a greater abundance of *Il1ra* and *Il18bp* transcripts in POP3-expressing mouse BMDMs infected with MVA than in their wild-type counterparts (**Supplementary Fig. 5f**). Thus, these studies of transgenic expression of POP3 in mouse macrophages further confirmed that POP3 had a role in inhibiting ALR-mediated release of cytokines, as initially observed by silencing of POP3 in human primary macrophages, and confirmed that human POP3 was functional in mice.

POP3 inhibits ALR-mediated caspase-1 activation in BMDMs

The PYDs of human and mouse ALRs are well conserved, and therefore it was not unexpected that in mouse BMDMs, POP3 also precipitated together with IFI16 and AIM2 but not with ASC (**Fig. 6a**), similar to the results we obtained with human THP-1 cells (**Fig. 2g**). As observed for human THP-1 cells, recombinant POP3 also weakly precipitated together with NLRP3 in BMDMs *in vitro* (**Fig. 6a**). That result further ensured that the function of human POP3 would be ‘translated’ to our mouse model. To delineate the mechanism by which POP3 inhibited ALR inflammasomes in mouse macrophages, we analyzed ASC oligomerization in response to stimulation of the AIM2 inflammasome with poly(dA:dT) in wild-type and CD68-POP3 BMDMs as a ‘readout’ of AIM2 inflammasome formation¹². Insoluble monomers, dimers and oligomers of ASC were much lower in abundance in the presence of POP3 (**Fig. 6b**), which supported the proposal of impaired formation of the AIM2 inflammasome in the presence of POP3. Inflammasome formation is essential for caspase-1 activation, and although the amount of pro-caspase-1 protein was not altered in POP3-expressing BMDMs, the abundance of the active p10 isoform of caspase-1 was much lower in culture supernatants of cells infected with MVA or MCMV but not those treated with LPS and ATP (**Fig. 6c**), which further emphasized the functional specificity of POP3 for formation of the AIM2 inflammasome but not for formation of the NLRP3 inflammasome. The effect of POP3 was specific for caspase-1 and was not caused by modulation of NF- κ B activation, since wild-type and CD68-POP3 cells had equal secretion of the NF- κ B-inducible cytokines TNF and IL-6 (**Fig. 5e,f**). In addition, we observed similar activation of NF- κ B and signaling via mitogen-activated protein kinase in BMDMs in response to infection with MVA in the absence and presence of POP3 (**Fig. 6d**). Furthermore, transcription of *Il1b*, *Il18*, *Ifnb*, *Asc*, *Aim2* and *Ifi16* was not lower in POP3-expressing BMDMs that were mock infected or infected with MVA than in wild-type BMDMs infected with MVA (**Fig. 6e**), which further supported the proposal of a role for POP3 in regulating AIM2-mediated inflammasome activation and caspase maturation but not in modulating the expression of inflammasome components. The finding of enhanced IFN- β production in POP3-expressing BMDMs was further supported by the finding of greater and more sustained phosphorylation of the transcription factor IRF3

Figure 6 POP3 interacts with AIM2 and IFI16

in BMDMs. **(a)** Precipitation of GST alone (negative control) or GST-POP3 together with endogenous proteins from total cell lysates of IFN- β -treated BMDMs, followed by immunoblot analysis (alongside total cell lysates without immunoprecipitation (TCL)). **(b)** Immunoblot analysis of ASC oligomerization in wild-type and CD68-POP3 BMDMs left untransfected (Ctrl) or transfected with poly(dA:dT) after crosslinkage of pellets (P), assessing inflammasome assembly. **(c)** Immunoblot analysis of pro-caspase-1 (Pro-casp1) in total cell lysates (TCL) and active caspase-1 (Casp1 p10) in supernatants (Sup) of wild-type and CD68-POP3 BMDMs mock infected or infected with MVA or MCMV or treated with LPS and ATP. **(d)** Immunoblot analysis of total and phosphorylated (p-) I κ B α (NF- κ B inhibitor), Jnk, p38 and p42/44 (mitogen-activated protein kinases) and IRF3 in total cell lysates of wild-type and CD68-POP3 BMDMs infected for various times (above lanes) with MVA, analyzed with 'pan-specific' and phosphorylation-specific antibodies. **(e)** Real-time PCR analysis of transcripts in wild-type and CD68-POP3 BMDMs before (Mock) and after (MVA) infection for 16 h with MVA. Data are representative of two experiments (error bars **(e)**, s.e.m. of three replicates).

in CD68-POP3 BMDMs in response to infection with MVA than in their wild-type counterparts (**Fig. 6d**). POP3 expression was much greater in response to infection with MVA (**Fig. 6e**), similar to the

expression of transcripts encoding the POP3-binding partners IFI16 and AIM2 and reminiscent of the results we obtained by immunoblot analysis of cells infected with MVA and treated with IFN- β (**Fig. 4d,e**).

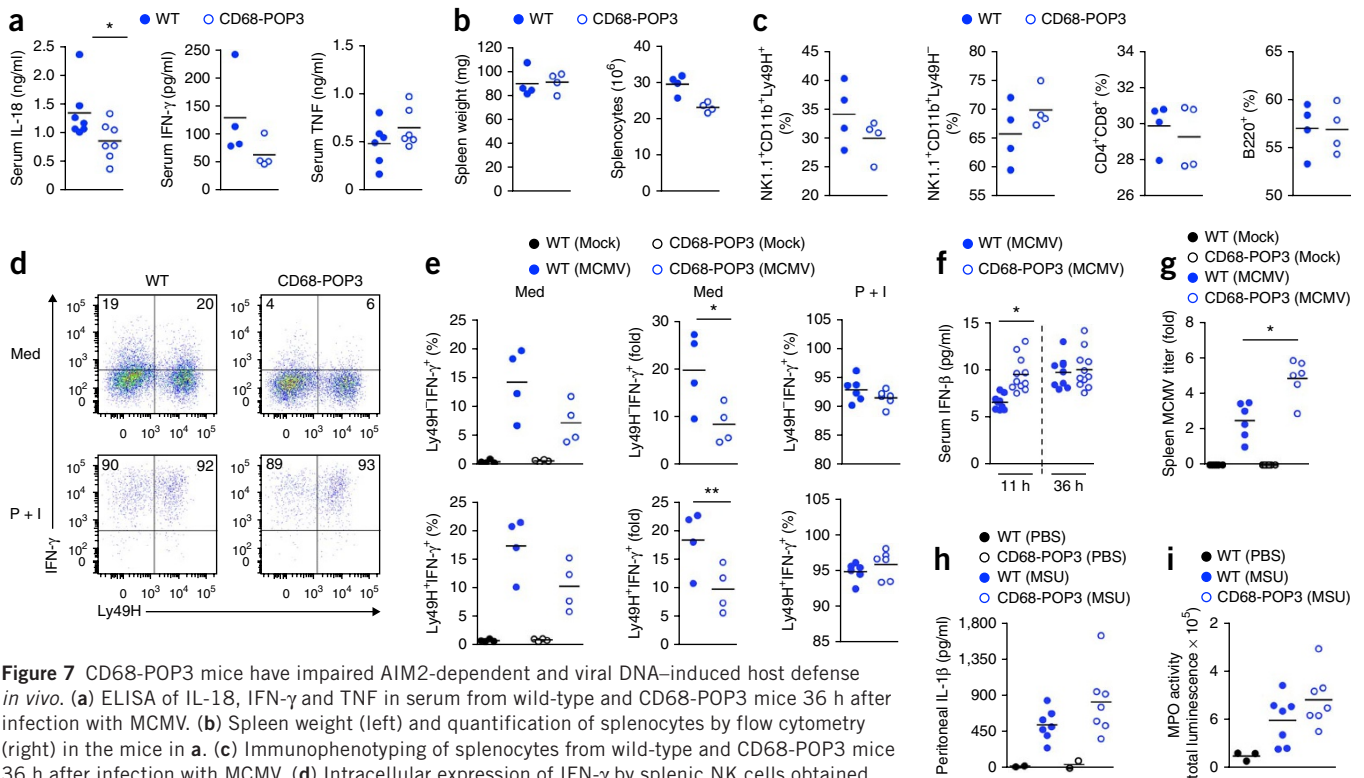


Figure 7 CD68-POP3 mice have impaired AIM2-dependent and viral DNA-induced host defense *in vivo*. **(a)** ELISA of IL-18, IFN- γ and TNF in serum from wild-type and CD68-POP3 mice 36 h after infection with MCMV. **(b)** Spleen weight (left) and quantification of splenocytes by flow cytometry (right) in the mice in **a**. **(c)** Immunophenotyping of splenocytes from wild-type and CD68-POP3 mice 36 h after infection with MCMV. **(d)** Intracellular expression of IFN- γ by splenic NK cells obtained from wild-type and CD68-POP3 mice 36 h after MCMV infection and cultured for 4 h *ex vivo* in medium alone (Med) or in the presence of PMA and ionomycin (P + I), gated on CD11b⁺NK1.1⁺ cells. Numbers in quadrants indicate percent Ly49H⁺IFN- γ ⁺ NK cells (top right) and Ly49H⁺IFN- γ ⁻ NK cells (top left). **(e)** Quantification of results in **d** for $n = 4$ –6 mice per group. **(f)** ELISA of IFN- β in serum from wild-type and CD68-POP3 mice 11 h or 36 h after infection with MCMV. **(g)** Splenic viral titers in wild-type and CD68-POP3 mice 7 h after intraperitoneal infection of PBS or MCMV. **(h)** ELISA of IL-1 β in peritoneal lavage fluid from wild-type and CD68-POP3 mice 7 h after intraperitoneal injection of PBS or MSU crystals. **(i)** Myeloperoxidase (MPO) activity in wild-type and CD68-POP3 mice 5 h after intraperitoneal injection of PBS or MSU crystals, assessed by *in vivo* imaging. Each symbol **(a–c, e–i)** represents an individual mouse; small horizontal lines indicate the mean. **(a)** * $P = 0.0451$. **(e)** * $P = 0.0457$ and ** $P = 0.0447$. **(f)** * $P = 0.0003$. **(g)** * $P = 0.0028$ (all two-tailed unpaired *t*-test). Data are representative of two experiments **(a–h)** or one experiment **(i)**.

These results demonstrated that POP3 affected cytokine release by inhibiting ALR-mediated activation of caspase-1.

POP3 blunts ALR-mediated antiviral host defense *in vivo*

Although there is support for the proposal of an inflammasome inhibitory role for POPs upon their overexpression, this has not been studied in macrophages or *in vivo*. *Aim2*^{-/-} mice have substantial impairment in mounting an efficient host response to infection with MCMV due to a deficiency in inflammasome-dependent systemic IL-18 release⁶. IL-18 acts in synergy with IL-12 to stimulate IFN- γ production by splenic NK cells, which is crucial for the early antiviral response to DNA viruses, including MCMV^{43,44}. Therefore, we challenged wild-type and CD68-POP3 mice with MCMV and found that, as in *Aim2* deficiency⁶, serum concentrations of IL-18 and IFN- γ were also much lower in CD68-POP3 mice than in their wild-type counterparts at 36 h after intraperitoneal infection (Fig. 7a). However, serum concentrations of TNF were not affected (Fig. 7a). After infection with MCMV, CD68-POP3 mice had a spleen weight similar to that of their wild-type counterparts but had slightly fewer splenocytes (Fig. 7b). Since IL-18 is required for the population expansion of Ly49H⁺ NK cells⁴⁵ and we had already observed lower IL-18 concentrations in CD68-POP3 mice (Fig. 7a), it was not unexpected that CD68-POP3 mice had fewer NK1.1⁺Ly49H⁺ cells but more NK1.1⁺Ly49H⁻ cells than their wild-type counterparts had (Fig. 7c). However, we found similar numbers of T cells and B cells in wild-type and CD68-POP3 mice (Fig. 7c and Supplementary Fig. 6). Accordingly, CD68-POP3 mice had significantly fewer IFN- γ -producing splenic NK cells *ex vivo* at 36 h after infection than did their wild-type counterparts (Fig. 7d,e), reminiscent of *Aim2*^{-/-} mice⁶. That response was specific to MCMV and was not due to an intrinsic defect in the ability of splenic NK cells from CD68-POP3 mice to produce IFN- γ , since activation of wild-type and CD68-POP3 splenic NK cells with the phorbol ester PMA and ionomycin *ex vivo* resulted in a similar frequency of IFN- γ ⁺ NK cells (~95%) (Fig. 7e). In addition to their impaired production of IL-18 and IFN- γ , CD68-POP3 mice had a higher serum concentration of IFN- β than that of wild-type mice at an early time point after infection with MCMV (11 h) but not at a later time point (36 h) (Fig. 7f). These results suggested that the deficient IFN- γ response was due to the diminished abundance of systemic IL-18 observed in CD68-POP3 mice upon infection with MCMV. IFN- γ is essential for restricting the amplification of MCMV *in vivo*; in agreement with that, we also observed a significantly greater splenic titer of MCMV in CD68-POP3 mice than in their wild-type counterparts (Fig. 7g). That twofold higher titer was similar to the twofold higher titer observed in *Asc*^{-/-} mice reported before⁶.

The proposal of functional specificity of POP3 for ALRs was further supported by the observation that wild-type and CD68-POP3 mice did not show a significant difference in their response to challenge with MSU crystals *in vivo*. The severity of MSU-induced peritonitis was similar in mice of both genotypes ($P = 0.1635$), with similar peritoneal concentrations of IL-1 β at 7 h after challenge with MSU ($P = 0.1308$) (Fig. 7h). Since IL-1 β produced by macrophages is essential for the infiltration of neutrophils into the peritoneal cavity⁴⁶, it was not unexpected that we observed no difference between wild-type and CD68-POP3 mice in their neutrophil infiltration *in vivo*, as assessed by a luminescent myeloperoxidase probe (Fig. 7i and Supplementary Fig. 7a). These results demonstrated that POP3 had a critical role in the host response to MCMV through regulating the AIM2 inflammasome *in vivo* without functionally affecting the NLRP3 inflammasome. Collectively, our data support a model in which POP3 functions

in the antiviral host response in a type I interferon-mediated inflammasome-regulatory feedback loop (Supplementary Fig. 7b).

DISCUSSION

Although inflammasome-produced cytokines are necessary for host defense and metabolic health, excessive and uncontrolled cytokine production contributes to pathological inflammation and autoinflammatory diseases. Hence, factors that promote a balanced inflammasome response are essential for maintaining homeostasis. However, the regulation of inflammasomes is still poorly understood. In particular, mechanisms for the discrimination between self DNA and foreign DNA have not been completely elucidated, but better understanding of this would delineate the underlying causes that contribute to the onset of autoinflammatory and autoimmune diseases, including systemic lupus erythematosus, Aicardi-Goutières syndrome and inflammatory myocarditis⁴⁷. Therefore, a control system that strictly and properly regulates DNA-induced immune responses is of utmost importance. Here we found that the type I interferon-inducible protein POP3 is one of the proteins that might function to maintain a balanced inflammasome response in humans by specifically inhibiting the assembly of ALR inflammasomes in response to immunogenic DNA. While other POPs directly interact with the inflammasome adaptor ASC^{18,19}, POP3 interacted with the PYD of ALRs and thereby prevented the recruitment of ASC. Although we found that recombinant POP3 interacted with NLRP3 *in vitro*, we did not observe functional impairment of NLRP3-dependent formation and activation of inflammasomes *in vitro* or *in vivo*. Notably, POP3 was not recruited to the endogenous ligand-induced NLRP3-ASC complex but was recruited to MVA-induced endogenous AIM2, where it prevented the recruitment of ASC. Thus, POP3 evolved as a specific regulator of ALR inflammasomes.

Our study further revealed that the human HIN-200 cluster is more complex than previously described and differs from that in mice. However, mice may use an alternative mechanism for regulating ALR inflammasomes through the DNA-binding HIN-200 family member p202, which lacks the PYD and is not expressed by humans but may function as an antagonist of AIM2 in mice¹⁴. However, p202 is barely detectable in C57BL/6 mice, which we used in our study here, but has high expression in BALB/c and NZB mouse strains¹⁴. This may have been an important influence on the ability of POP3 expression in C57BL/6 mice to substantially alter the immune response upon MCMV infection in our study of 'humanized' C57BL/6 mice. In mice, two genes that encode only a PYD are predicted to be in the HIN-200-encoding cluster; both of these lack a human ortholog. *Pydc3* (*Ifi208*) is predicted to encode only a PYD but is much larger than POP-encoding genes and might encode a HIN-200 domain, according to analysis of expressed sequence tags^{16,34}. Two predicted alternative transcripts of *Pydc4* encode only a PYD³⁴, but the longest transcript encodes a 586-amino acid protein that is 95.2% identical to PYDC3. However, neither gene shows similarity to POP3 and no expression data or functional data are available³⁴. *Aim2b*, a predicted splice form of *Aim2* in mice, might encode a protein whose function most closely resembles that of POP3 in mice. Similar to the locus encoding human HIN-200, the chromosomal region encoding rat HIN-200 is also predicted to contain genes (*Rhin2*, *Rhin3*, *Rhin4* and *Aim2*) that encode four HIN-200 proteins and the putative POP-encoding gene *Rhin5*, which is twice the size of POP3 and shares less than 14% sequence identity and also lacks any expression data³⁴. We speculate that contrary to its evolution in mice, POP3 evolved in humans to interfere with the assembly of ALR inflammasomes.

Its type I interferon responsiveness further distinguishes POP3 from other members of the POP family. Thus, POP3 represents one of the type I interferon-inducible proteins that antagonizes IFN- γ in macrophages and inflammasome activation⁴⁰ and might contribute to the anti-inflammatory and immunosuppressive functions of type I interferons⁴⁸. *Aim2*^{-/-} BMDMs showed elevated IFN- β production, although the mechanism by which AIM2 negatively regulates IFN- β production is unknown^{5,6}. However, we observed that silencing of POP3, which increased AIM2 signaling, also reduced the production of IFN- β and, accordingly, we found that POP3 expression in human primary macrophages, THP-1 cells and BMDMs promoted IFN- β production. Thus, in addition to promoting its own IFN- β -dependent production, POP3 might shift the immune response from inflammasome-dependent proinflammatory cytokine production to anti-inflammatory IFN- β production and thereby further blunt signaling via IL-1 β and IL-18 through upregulation of the expression of IL-1RA and IL-18BP^{41,42}. A similar mechanism has been proposed for LRRFP2, which inhibits activation of the NLRP3 inflammasome by recruiting the pseudo-caspase-1 substrate flightless-1⁴⁹ but also functions as a sensor of cytosolic DNA that promotes the production of type I interferons⁵⁰. Notably, we observed the IFN- β -inducible expression pattern of POP3 as an early and late response in CD68-POP3 mice. Thus, our humanized mouse represents a model with which to study inflammasome regulation *in vivo* and probably reflects POP3 functions in humans. Thus, it is possible that POP3 might also contribute to the amelioration of DNA-driven autoimmune disease. Although mice lack POP3, macrophage-specific transgenic expression of POP3 revealed that POP3 is nevertheless functional in mice. Our study represents the first *in vivo* study of any member of the POP family, to our knowledge. Although inflammasomes have been reported in various cell types, their relative importance in IL-1 β - and IL-18-dependent host responses *in vivo* have not been studied. Our study also represents the first macrophage-specific mouse model for the study of inflammasomes, to our knowledge, for investigating the role of macrophages in this response, and emphasizes their key role in DNA virus-induced inflammasome activation.

METHODS

Methods and any associated references are available in the [online version of the paper](#).

Accession codes. GenBank/EMBL/DDBJ: gene data, [KF562078](#).

Note: Any Supplementary Information and Source Data files are available in the online version of the paper.

ACKNOWLEDGMENTS

We thank B.C. Schaefer (Uniformed Services University of the Health Sciences) for the promoter of the gene encoding ubiquitin C; J. DeGregori (University of Colorado Health Sciences Center) for the plasmid pLXS-hCAR^{Δcyt}; D. Trono (École Polytechnique Fédérale de Lausanne) for plasmids pMD2.G and psPAX2; K.A. Fitzgerald (University of Massachusetts) for *Aim2*^{-/-} mice; the Northwestern University Transgenic and Targeted Mutagenesis Laboratory for assistance in generating transgenic mice; and A.D. Radian for the isolation of human macrophages. Supported by the US National Institutes of Health (GM071723, HL097183, AI092490, AI082406, AI099009 and AR064349 to C.S.; AR057532 to A.D., AR050250, AR054796, AI092490 and HL108795 to H.P.; AR064313 to C.M.C.; and T32AR007611 to L.d.A.), the National Cancer Institute (CA060553), the National Institute of Arthritis and Musculoskeletal and Skin Diseases (AR057216), the American Heart Association (12GRNT12080035 to C.S.), the Arthritis Foundation (AF161715 to S.K.), the American Heart Association (11POST585000 to L.d.A.) and the Solovy/Arthritis Research Society (H.P.).

AUTHOR CONTRIBUTIONS

A.D. and C.S. designed the research; S.K., R.A.R., L.d.A., C.M.C., S.L.R., A.V.M., M.C.W. and A.G. did experiments; E.F., E.G., H.P., J.C.R. and D.R.G. provided

reagents, expertise and advice; S.K., R.A.R., L.d.A., C.M.C., A.V.M., H.P., A.D. and C.S. analyzed results; S.K., A.D. and C.S. wrote the paper; and A.D. and C.S. conceived of the study, designed the experiments and provided overall direction.

COMPETING FINANCIAL INTERESTS

The authors declare no competing financial interests.

Reprints and permissions information is available online at <http://www.nature.com/reprints/index.html>.

- Martinon, F., Burns, K. & Tschopp, J. The Inflammasome: A molecular platform triggering activation of inflammatory caspases and processing of proIL-1 β . *Mol. Cell* **10**, 417–426 (2002).
- Stehlik, C. *et al.* Apoptosis-associated speck-like protein containing a caspase recruitment domain is a regulator of procaspase-1 activation. *J. Immunol.* **171**, 6154–6163 (2003).
- Srinivasula, S.M. *et al.* The PYRIN-CARD protein ASC is an activating adaptor for Caspase-1. *J. Biol. Chem.* **277**, 21119–21122 (2002).
- Barbalat, R., Ewald, S.E., Mouchess, M.L. & Barton, G.M. Nucleic acid recognition by the innate immune system. *Annu. Rev. Immunol.* **29**, 185–214 (2011).
- Fernandes-Alnemri, T. *et al.* The AIM2 inflammasome is critical for innate immunity to *Francisella tularensis*. *Nat. Immunol.* **11**, 385–393 (2010).
- Rathinam, V.A. *et al.* The AIM2 inflammasome is essential for host defense against cytosolic bacteria and DNA viruses. *Nat. Immunol.* **11**, 395–402 (2010).
- Jones, J.W. *et al.* Absent in melanoma 2 is required for innate immune recognition of *Francisella tularensis*. *Proc. Natl. Acad. Sci. USA* **107**, 9771–9776 (2010).
- Kerur, N. *et al.* IFI16 acts as a nuclear pathogen sensor to induce the inflammasome in response to kaposi sarcoma-associated herpesvirus infection. *Cell Host Microbe* **9**, 363–375 (2011).
- Albrecht, M., Choubey, D. & Lengauer, T. The HIN domain of IFI-200 proteins consists of two OB folds. *Biochem. Biophys. Res. Commun.* **327**, 679–687 (2005).
- Jin, T. *et al.* Structures of the HIN domain:DNA complexes reveal ligand binding and activation mechanisms of the AIM2 inflammasome and IFI16 receptor. *Immunity* **36**, 561–571 (2012).
- Bürckstümmer, T. *et al.* An orthogonal proteomic-genomic screen identifies AIM2 as a cytoplasmic DNA sensor for the inflammasome. *Nat. Immunol.* **10**, 266–272 (2009).
- Fernandes-Alnemri, T., Yu, J.W., Datta, P., Wu, J. & Alnemri, E.S. AIM2 activates the inflammasome and cell death in response to cytoplasmic DNA. *Nature* **458**, 509–513 (2009).
- Hornung, V. *et al.* AIM2 recognizes cytosolic dsDNA and forms a caspase-1-activating inflammasome with ASC. *Nature* **458**, 514–518 (2009).
- Roberts, T.L. *et al.* HIN-200 proteins regulate caspase activation in response to foreign cytoplasmic DNA. *Science* **323**, 1057–1060 (2009).
- Schattgen, S.A. & Fitzgerald, K.A. The PYHIN protein family as mediators of host defenses. *Immunol. Rev.* **243**, 109–118 (2011).
- Ludlow, L.E., Johnstone, R.W. & Clarke, C.J. The HIN-200 family: more than interferon-inducible genes? *Exp. Cell Res.* **308**, 1–17 (2005).
- Dorfleutner, A. *et al.* A Shope fibroma virus PYRIN-only protein modulates the host immune response. *Virus Genes* **35**, 685–694 (2007).
- Dorfleutner, A. *et al.* Cellular pyrin domain-only protein 2 is a candidate regulator of inflammasome activation. *Infect. Immun.* **75**, 1484–1492 (2007).
- Stehlik, C. *et al.* The PAAD/PYRIN-only protein POP1/ASC2 is a modulator of ASC-mediated NF- κ B and pro-caspase-1 regulation. *Biochem. J.* **373**, 101–113 (2003).
- Stehlik, C. & Dorfleutner, A. COPs and POPs: modulators of inflammasome activity. *J. Immunol.* **179**, 7993–7998 (2007).
- Bedoya, F., Sandler, L.L. & Harton, J.A. Pyrin-only protein 2 modulates NF- κ B and disrupts ASC:CLR interactions. *J. Immunol.* **178**, 3837–3845 (2007).
- Johnston, J.B. *et al.* A poxvirus-encoded pyrin domain protein interacts with ASC-1 to inhibit host inflammatory and apoptotic responses to infection. *Immunity* **23**, 587–598 (2005).
- Hiller, S. *et al.* NMR Structure of the apoptosis- and inflammation-related NALP1 pyrin domain. *Structure* **11**, 1199–1205 (2003).
- Jin, T., Perry, A., Smith, P., Jiang, J. & Xiao, T.S. Structure of the absent in melanoma 2 (AIM2) pyrin domain provides insights into the mechanisms of AIM2 autoinhibition and inflammasome assembly. *J. Biol. Chem.* **288**, 13225–13235 (2013).
- Boyden, E.D. & Dietrich, W.F. Nalp1b controls mouse macrophage susceptibility to anthrax lethal toxin. *Nat. Genet.* **38**, 240–244 (2006).
- Faustin, B. *et al.* Reconstituted NALP1 inflammasome reveals two-step mechanism of caspase-1 activation. *Mol. Cell* **25**, 713–724 (2007).
- Martinon, F., Petrilli, V., Mayor, A., Tardivel, A. & Tschopp, J. Gout-associated uric acid crystals activate the NALP3 inflammasome. *Nature* **440**, 237–241 (2006).
- Cassel, S.L. *et al.* The Nalp3 inflammasome is essential for the development of silicosis. *Proc. Natl. Acad. Sci. USA* **105**, 9035–9040 (2008).
- Dostert, C. *et al.* Innate immune activation through Nalp3 inflammasome sensing of asbestos and silica. *Science* **320**, 674–677 (2008).
- Hornung, V. *et al.* Silica crystals and aluminum salts activate the NALP3 inflammasome through phagosomal destabilization. *Nat. Immunol.* **9**, 847–856 (2008).

31. Franchi, L. *et al.* Cytosolic flagellin requires Ipaf for activation of caspase-1 and interleukin 1 β in salmonella-infected macrophages. *Nat. Immunol.* **7**, 576–582 (2006).
32. Miao, E.A. *et al.* Cytoplasmic flagellin activates caspase-1 and secretion of interleukin 1 β via Ipaf. *Nat. Immunol.* **7**, 569–575 (2006).
33. Unterholzner, L. *et al.* IFI16 is an innate immune sensor for intracellular DNA. *Nat. Immunol.* **11**, 997–1004 (2010).
34. Cridland, J.A. *et al.* The mammalian PYHIN gene family: phylogeny, evolution and expression. *BMC Evol. Biol.* **12**, 140 (2012).
35. Gough, P.J., Gordon, S. & Greaves, D.R. The use of human CD68 transcriptional regulatory sequences to direct high-level expression of class A scavenger receptor in macrophages *in vitro* and *in vivo*. *Immunology* **103**, 351–361 (2001).
36. Greaves, D.R., Quinn, C.M., Seldin, M.F. & Gordon, S. Functional comparison of the murine macrophage and human CD68 promoters in macrophage and nonmacrophage cell lines. *Genomics* **54**, 165–168 (1998).
37. Mariathasan, S. *et al.* Cryopyrin activates the inflammasome in response to toxins and ATP. *Nature* **440**, 228–232 (2006).
38. Leon, R.P. *et al.* Adenoviral-mediated gene transfer in lymphocytes. *Proc. Natl. Acad. Sci. USA* **95**, 13159–13164 (1998).
39. Schaefer, B.C., Schaefer, M.L., Kappler, J.W., Marrack, P. & Kedl, R.M. Observation of antigen-dependent CD8⁺ T-cell/dendritic cell interactions *in vivo*. *Cell. Immunol.* **214**, 110–122 (2001).
40. Guarda, G. *et al.* Type I interferon inhibits interleukin-1 production and inflammasome activation. *Immunity* **34**, 213–223 (2011).
41. Kaser, A. *et al.* Interferon-alpha induces interleukin-18 binding protein in chronic hepatitis C patients. *Clin. Exp. Immunol.* **129**, 332–338 (2002).
42. Sciacca, F.L., Canal, N. & Grimaldi, L.M. Induction of IL-1 receptor antagonist by interferon β : implication for the treatment of multiple sclerosis. *J. Neurovirol.* **6** (suppl. 2), S33–S37 (2000).
43. Pien, G.C., Satoskar, A.R., Takeda, K., Akira, S. & Biron, C.A. Cutting edge: selective IL-18 requirements for induction of compartmental IFN- γ responses during viral infection. *J. Immunol.* **165**, 4787–4791 (2000).
44. Smith, H.R.C. *et al.* Recognition of a virus-encoded ligand by a natural killer cell activation receptor. *Proc. Natl. Acad. Sci. USA* **99**, 8826–8831 (2002).
45. Andrews, D.M., Scalzo, A.A., Yokoyama, W.M., Smyth, M.J. & Degli-Esposti, M.A. Functional interactions between dendritic cells and NK cells during viral infection. *Nat. Immunol.* **4**, 175–181 (2003).
46. McDonald, B. *et al.* Intravascular danger signals guide neutrophils to sites of sterile inflammation. *Science* **330**, 362–366 (2010).
47. Pisetsky, D.S. The role of innate immunity in the induction of autoimmunity. *Autoimmun. Rev.* **8**, 69 (2008).
48. González-Navajas, J.M., Lee, J., David, M. & Raz, E. Immunomodulatory functions of type I interferons. *Nat. Rev. Immunol.* **12**, 125–135 (2012).
49. Jin, J. *et al.* LRRFIP2 negatively regulates NLRP3 inflammasome activation in macrophages by promoting Flightless-I-mediated caspase-1 inhibition. *Nat. Commun.* **4**, 2075 (2013).
50. Yang, P. *et al.* The cytosolic nucleic acid sensor LRRFIP1 mediates the production of type I interferon via a β -catenin-dependent pathway. *Nat. Immunol.* **11**, 487–494 (2010).

ONLINE METHODS

Mice. Plasmid pCD68-POP3 was generated by replacement of the sequence encoding chloramphenicol acetyltransferase in the plasmid pCAT-Basic (which contains the promoter of the gene encoding human CD68 and the macrophage-specific IVS-1 enhancer^{37,38}) with sequence encoding human POP3, as well as flanking of that cassette with *AatII* restriction sites. The *AatII* fragment was excised and purified, and transgenic mice (B6.TgN(CD68-POP3)) were generated by pronuclear injection of that fragment into C57BL/6 embryos. Two lines were initially analyzed, and subsequently a single line was used for most experiments; genotyping was outsourced to Transnetyx. Transgenic mice with expression of the human coxsackie and adenovirus receptor lacking the cytoplasmic domain from the ubiquitin C gene (B6.TgN(*UbiC-hCAR*) mice) were generated by pronuclear injection of a *BglII* fragment from the plasmid pUBI containing the promoter and intron of the gene encoding ubiquitin C⁴¹ plus the human coxsackie and adenovirus receptor with deletion of the cytoplasmic domain⁴⁰. Mice were housed in a specific pathogen-free animal facility and all experiments used age- and sex-matched mice 8–12 weeks of age and were conducted according to procedures approved by the Northwestern University Committee on Use and Care of Animals.

Isolation, culture and transfection of macrophages. After informed consent was obtained, blood was obtained from healthy donors by a protocol approved by Northwestern University Institutional Review Board Human, then primary macrophages were isolated from the blood by Ficoll-Hypaque centrifugation (Sigma) and countercurrent centrifugal elutriation in the presence of 10 µg/ml polymyxin B with a JE-6B rotor (Beckman Coulter), as described⁵¹. Cells in 24-well dishes (2.5 × 10⁵ cells per well) were transfected with 120 nM siRNA duplexes (POP3-specific Stealth siRNA (sense, 5'-CAUGGCAUUCUGGGAAUGCAUGUU-3') POP3-specific siRNA#2 (sense, 5'-GAGCAGGAAACGGUAUAUGUGGGA-3') or control stealth siRNA; both from Invitrogen) through the use of F2 reagent plus Virofect (Targeting Systems) and were analyzed 72 h later, as described⁵¹. BMDMs were flushed from femurs and tibia, then were differentiated in conditioned medium from L929 mouse fibroblasts (25%) in DMEM supplemented with 10% heat inactivated FCS (Invitrogen) and analyzed after 7 d. Resting or elicited peritoneal macrophages were isolated by peritoneal lavage before or 3–5 d after intraperitoneal injection of 1 ml of 4% aged thioglycollate medium. THP-1 cells from American Type Culture Collection were routinely tested for mycoplasma contamination. THP-1 cells were stably transduced with pLEX-based lentiviral particles. Human primary macrophages, THP-1 cells, BMDMs and peritoneal macrophages were treated for various times with 600 ng/ml *Escherichia coli* LPS (0111:B4; Sigma) or were pretreated with ultrapure *E. coli* LPS (100 ng/ml; 0111:B4; Invitrogen), MSU (400 ng/ml; Invitrogen), mouse and human IFN-β (1,500 U/ml; Millipore), MG132 (10 µM; Calbiochem), mouse IL-1Ra (100 ng/ml; R&D Systems) or recombinant IL-1Ra (anakinra; 10 mg/ml; Amgen). Cells were transfected with poly(dA:dT) (2 ng/ml; Sigma), muramyl dipeptide (20 µg/ml; Invitrogen), *Salmonella thymurium* flagellin (140 ng/ml; Invitrogen) and *B. anthracis* lethal toxin and protective antigen (1 µg/ml; List Biological Laboratories) through the use of Lipofectamine 2000 (Invitrogen). Where appropriate, cells were pulsed for 20 min with ATP (5 mM; Sigma) or treated for 45 min with nigericin (5 µM).

Preparation of virus. Recombinant adenovirus was generated by cloning of sequence encoding GFP or GFP-POP3 into the plasmid pShuttle, followed by recombination with pAdEasy in *E. coli* BJ5183 and purification from the HEK293N subtype of HEK293 cells on a cesium-chloride gradient. Lentiviral particles were generated in HEK293T-Lenti cells (Clontech) transfected with pLEX containing sequence encoding GFP or GFP-POP3 and the packaging plasmids pMD.2G and pSPAX2 (12259 and 12260; Addgene). MCMV, Smith strain (VR-1399; American Type Culture Collection) was propagated in SG-1 mouse embryo fibroblast (CRL-1404; American Type Culture Collection) for cell-based experiments and was passaged twice for 2 weeks each in the salivary glands of 6- to 8-week-old BALB/c mice after intraperitoneal injection of MCMV (1.5 × 10⁵ plaque-forming units (PFU) per ml). Mice were killed and then salivary glands were collected, homogenized in Hank's balanced-salt solution and clarified and viral titers were determined by plaque-formation assay

and a Taqman quantitative PCR assay based on the MCMV immediate-early gene and gene encoding glycoprotein B (Invitrogen) with a standard curve for MCMV. MCMV was then stored in aliquots at -80 °C. Clarified salivary gland homogenates from uninfected mice were used for mock infection. Macrophages in 24-well plates (2.5 × 10⁵ cells per well) were infected with MCMV (1 × 10⁵ PFU per well). MVA (VR-1508; American Type Culture Collection) was amplified in BHK-21 hamster fibroblasts (CCL-10; American Type Culture Collection). MVA titers were determined by a plaque-forming assay in BHK-21 cells. Macrophages in 24-well plates (2.5 × 10⁵ cells per well) were infected with MVA (1 × 10⁶ PFU per well). The KSHV lytic cycle was induced from the BCBL-1 human lymphoma cell line by supplementation of the medium with TPA (12-O-tetradecanoylphorbol-13-acetate; 20 ng/ml). KSHV-containing culture supernatants were collected after 96 h, then were clarified by centrifugation (330g for 5 min, followed by centrifugation at 1,540g for 30 min) and were filtered through filters with a pore size of 0.45 µm. KSHV was subsequently concentrated by ultracentrifugation at 20,000 r.p.m. for 90 min (SW28 rotor; 4 °C). Viral pellets were resuspended in EBM2 medium (Lonza), filtered through filters with a pore size of 0.45 µm and titered on iHMVEC endothelial cells⁵². KSHV was used to infect 2.5 × 10⁵ macrophages at an infectivity of 1.2 × 10⁵ transduction units per 24-well plate.

Plasmids. The pCDNA3-based expression constructs for ASC, POP1 and POP2 have been described^{17–19,51,53,54}. Sequence encoding POP3 (GenBank/EMBL/DDBJ accession code, [KF562078](#)), AIM2, the AIM2 PYD, IFI16, the IFI16 PYD, IFIX, the IFIX PYD, MNDA or the MNDA PYD was generated by standard PCR from cDNA and expressed sequence tags (Open Biosystems), then the cDNA was cloned in pCDNA3, pLEX or pShuttle with an amino-terminal c-Myc, hemagglutinin, Flag, GFP or RFP tag. The sequences of all expression constructs were verified.

Immunoblot analysis, immunoprecipitation and immunohistochemistry. Rabbit polyclonal and mouse monoclonal antibodies to POP3 were 'custom raised' (keyhole limpet hemocyanin-conjugated CGSPSSARSVSQSL). Other antibodies for immunoblot analysis were as follows: rabbit polyclonal antibody to ASC (clone 2EI-7; Chemicon; and 'custom raised'); mouse monoclonal antibody to ASC ('custom raised'); mouse polyclonal antibody to caspase-1 (M-20), mouse monoclonal antibody to the human coxsackie and adenovirus receptor (Mab.E[mh1]), mouse monoclonal antibody to GFP (B-2), mouse monoclonal antibody to dsRED (F-9), mouse monoclonal antibody to the amino terminus of IFI16 (1G7), mouse monoclonal antibody to β-tubulin (TU-02) and mouse monoclonal antibody to GST (B-14; all from Santa Cruz Biotech); mouse monoclonal antibody to c-Myc (9E10; Roche and Santa Cruz Biotech); mouse monoclonal antibody to the carboxyl terminus of IFI16 (ab104409; Abcam); rabbit polyclonal antibody to the carboxyl terminus of AIM2 (8055; Cell Signaling Technology); rabbit polyclonal antibody to IκBα (44D4), antibody to phosphorylated IκBα (14D4), anti-Jnk (9252), antibody to phosphorylated JNK (9251), anti-p38 (9212), antibody to phosphorylated p38 (12F8), to p42/44 (9102), antibody to phosphorylated p42/44 (9101), anti-IRF3 (D83B9) and antibody to phosphorylated IRF3 (4D4G; all from Cell Signaling Technology); and mouse monoclonal antibody to NLRP3 (Cryo-2; Adipogen). For coimmunoprecipitation, HEK293 cells in 100-mm dishes were transfected with plasmid encoding GFP-POP3, hemagglutinin-tagged ASC, RFP-tagged AIM2 or empty plasmid (Lipofectamine 2000; Invitrogen). Cells were lysed (50 mM HEPES, pH 7.4, 150 mM NaCl, 10% Glycerol, 2 mM EDTA and 0.5% Triton X-100, supplemented with protease inhibitors) 36 h after transfection. Cleared lysates were subjected to immunoprecipitation by incubation for 16 h at 4 °C with immobilized antibodies, followed by extensive washing with lysis buffer. Bound proteins were separated by SDS-PAGE, transferred to PVDF membranes and analyzed by immunoblot with the appropriate primary antibodies and horseradish peroxidase-conjugated secondary antibodies (whole donkey antibody to rabbit IgG (NA934V) and whole sheep antibody to mouse IgG (NXA931); both from GE Healthcare), ECL detection (Pierce) and image acquisition (Ultralum). Total cell lysate (5%) were also analyzed where necessary. Endogenous NLRP3 and AIM2 inflammasome complexes were similarly purified from THP-1 cells primed for 16 h with ultrapure LPS (100 ng/ml), followed by treatment for 45 min with nigericin (5 µM) or infection for 90 min

with MVA, respectively. For GST precipitation experiments, sequence encoding POP3 was cloned into plasmid pGEX-4T1, followed by affinity purification from *E. coli* BL21 as a GST fusion protein. Proteins were prepared by *in vitro* transcription and translation (TNT Quick Coupled Transcription/Translation; Promega) or total cell lysate were prepared from IFN- β -treated (16 h) BMDM or THP-1 cells by lysis (50 mM HEPES, pH 7.4, 120 mM NaCl, 10% glycerol, 2 mM EDTA and 0.5% Triton X-100, supplemented with protease inhibitors) as a source of endogenous proteins, and cleared lysates were incubated for 16 h at 4 °C with immobilized GST-POP3 or GST-only control, followed by extensive washing with lysis buffer and analysis as described above. For crosslinkage of ASC, 4×10^6 BMDMs were seeded in 60-mm plates and subjected to crosslinking as described⁵⁵. Cells were transfected for 5 h with 1 μ g/ml poly(dA:dT), then supernatants were removed and cells were rinsed with ice-cold PBS and lysed (20 mM HEPES, pH 7.4, 100 mM NaCl, 1% NP-40 and 1 mM sodium orthovanadate, supplemented with protease inhibitors) and further lysed by shearing. Cleared lysates were stored for immunoblot analysis and the insoluble pellets were resuspended in 500 μ l PBS supplemented with 2 mM DSS (disuccinimidyl suberate; Pierce) and incubated with rotation for 30 min at room temperature. Samples were centrifuged at 5,000 r.p.m. for 10 min at 4 °C and the crosslinked pellets were resuspended in 50 μ l Laemmli sample buffer and analyzed by immunoblot. Human lung tissue was embedded in paraffin, cut into sections 3 μ m in thickness, mounted, deparaffinized and immunostained with mouse monoclonal antibody to CD68 (Dako) and rabbit polyclonal antibody to POP3 ('custom-raised'), the enzyme-chromogen combinations horseradish peroxidase-3,3'-diaminobenzidine tetrahydrochloride and alkaline phosphatase-Fast Red (Dako) and specific isotype-matched control antibodies (mouse IgG1 κ -chain (X0931; Dako) and rabbit IgG (X0903; Dako)) with hematoxylin counterstaining of nuclei.

Immunofluorescence microscopy. Human primary macrophages grown on cover slips were treated for 16 h with IFN- β or were infected with adenovirus expressing GFP or GFP-POP3 or were infected for 2 h with MVA or for 8 h with KSHV, then were fixed and permeabilized and then immunostained with anti-AIM2 (8055; Cell Signaling), anti-IFI16 (IG7; Santa Cruz Biotech) and anti-POP3 ('custom raised') and Alexa Fluor-conjugated secondary antibodies (Alexa Fluor 546-conjugated goat antibody to rabbit IgG (A11035; Molecular Probes) and Alexa Fluor 488-conjugated goat antibody to mouse IgG (A11029; Molecular Probes)), with counterstaining of nuclei with DAPI (4,6-diamidino-2-phenylindole; Invitrogen)⁵⁴. Images were acquired by fluorescence microscopy on a Nikon TE2000E2-PFS with a 100 \times oil objective and image deconvolution (Nikon Elements).

Measurement of cytokines and caspase-1. IL-1 β , IL-18, TNF, IL-6, IFN- β and IFN- γ were quantified by ELISA (BD Biosciences, eBiosciences and Invitrogen) in clarified culture supernatants of human primary macrophages, BMDMs and peritoneal macrophages and in mouse serum. Samples were analyzed in triplicates and analyses were repeated at least three times. Active caspase-1 p10 was detected by immunoblot analysis of TCA-precipitated serum-free culture supernatants 4 h after treatment⁵¹.

mRNA analysis. Expression of mRNA from target genes was quantified by RT-PCR or *in vivo* by with gold nanoparticles conjugated to specific oligonucleotides in duplex with indodicarbocyanine-labeled reporter strands, which are nontoxic and are endocytosed by live cells (SmartFlares; Millipore). Flow cytometry in combination with lineage specific markers was used for subsequent analysis. For this, 7- to 12-week-old mice received an intraperitoneal injection of MCMV (10^5 PFU) for 6 h. Mice were killed and peritoneal cells were obtained by lavage. Retro-orbital blood was collected in EDTA-containing tubes, followed by incubation for 16 h with control or POP3-specific SmartFlare strands (1:1,000 dilution in Hanks balanced-salt solution). Subsequently, non-specific binding in cells was blocked with Fc-Block (2.4G2; BD), then cells were stained with fluorochrome-conjugated antibodies (identified below) and fixed and samples were depleted of red blood cells with BD FACS Lysing solution (BD Biosciences), followed by analysis on an LSR II (BD). Data were compensated and evaluated with FlowJo software (TreeStar). Doublets and debris were excluded and leukocytes were identified with the pan-hematopoietic

marker anti-CD45 (30-F11; BD). Leukocyte subsets were identified by positive staining with the following antibodies: CD4⁺ T cells, anti-CD4 (RM4-5; BD); CD8⁺ T cells, anti-CD8 (53-6.7; BD); B cells, anti-B220 (RA3-6B2; BD); NK cells, anti-NK1.1 (PK-136, BD); neutrophils, anti-CD11b (M1/70; eBioscience) and anti-Ly6G (1A8; BD); monocytes, anti-CD11b (M1/70; eBioscience) and anti-Ly-6C (AL-21; BD); and macrophages, anti-CD11b (M1/70; eBioscience) and anti-F4/80 (BM8; eBioscience). Monocytes were further subcategorized as Ly-6C^{hi} classical or inflammatory monocytes and Ly-6C^{lo-med} nonclassical or resident monocytes. Total RNA was isolated from human primary macrophages, BMDMs or mouse blood with Trizol (Invitrogen) or a mouse RiboPure-blood RNA isolation kit (Invitrogen), then RNA was treated with DNase I, reverse-transcribed with GoScript (Promega) and analyzed with a TaqMan Real-time gene-expression system with pre-designed 5-carboxyfluorescein-labeled primers and probes on an ABI 7300 Real Time PCR device (Applied Biosystems); results are presented relative to those of genes encoding GAPDH (glyceraldehyde phosphate dehydrogenase) or β -actin. The POP3 TaqMan assay was custom designed as follows: forward, 5'-AGCACGAGTAGCCAACCTTGATT-3'; reverse, 5'-GGTCTTCCTCACTGCAGACA-3'; and 5-carboxyfluorescein-labeled probe, 5'-CCATGCCAGCGTTT-3'. The RT-PCR primers for POP3 were as follows: forward, 5'-ATGGAGAGTAAATATAAGGAG-3', and reverse, 5'-TCAACATGCATTCCCAGAAAT-3'.

***In vivo* virus infection and intracellular IFN- γ staining.** 8- to 10-week-old age- and sex-matched wild-type and CD68-POP3 mice were randomly assigned to groups to be infected with 1×10^5 to 1×10^6 PFU of MCMV or to undergo mock infection, each by intraperitoneal injection. Salivary gland homogenates were obtained and mice were killed after 36 h. Spleens were digested for 15 min at 37 °C with collagenase type D (1 mg/ml; Roche) and DNase I (0.1 mg/ml; Roche) in Hank's balanced-salt solution, then were passed through 40- μ m nylon cell strainers (BD Biosciences), after which red cells were lysed with 1 \times BD Pharm Lyse buffer (BD Biosciences) and samples were washed with complete RPMI medium (RPMI-1640 medium with 10% FCS, 2 mM glutamine, 100 U/ml penicillin, 0.1 mg/ml streptomycin, 10 mM HEPES buffer and 1 mM sodium pyruvate). Splenocytes were counted (Countess cell counter; Invitrogen), and 3×10^6 splenocytes were directly stained for IFN- γ expression, and an additional 3×10^6 splenocytes were first suspended in complete RPMI medium and then were stimulated for 4 h in the presence of leukocyte-activation 'cocktail' (2 μ l/ml, BD Biosciences) before being stained⁶. Splenocytes were preincubated with mouse Fc block and were labeled with predetermined optimal concentrations of fluorescence-labeled anti-B220, anti-CD4, anti-CD8, anti-CD11b, anti-CD69 and anti-NK1.1 (all identified above) and anti-Ly49H (3D10; eBioscience). A Cytotfix/Cytoperm Kit was used according to the manufacturer's specifications (BD Biosciences) for intracellular staining with anti-IFN- γ (XMG1.2; eBioscience), and dead cells were excluded with Aqua Live/Dead stain (Invitrogen). At least 4×10^5 events per sample were acquired on an LSR II (BD), and data were analyzed with FlowJo software (TreeStar).

MSU-induced peritonitis. 10- to 12-week-old age- and sex-matched wild-type and CD68-POP3 mice were randomly assigned to groups to receive intraperitoneal injection of PBS (0.5 ml per mouse) or MSU crystals in PBS (10 mg in 0.5 ml PBS per mouse). At 5 h after that injection, mice were given intraperitoneal injection of the luminescent Xenolight Rediject Inflammation probe (200 mg per kg body weight; PerkinElmer)⁵⁶. Images were exposed for 5 min (IVIS Spectrum; PerkinElmer) and luminescence was quantified with Living Image (PerkinElmer). Mice were also killed 7 h after injection of PBS or MSU and peritoneal cavities were flushed with 2 ml ice-cold PBS with 10% FBS, then the fluid was clarified by centrifugation and IL-1 β was analyzed by ELISA.

Statistics. A standard two-tailed unpaired *t*-test (Prism 5; GraphPad) was used for statistical analysis of two groups with all data points showing a normal distribution, and *P* values of <0.05 were considered significant. The investigators were not 'blinded' to the genotype of the mice or cells. Sample sizes were selected on the basis of preliminary results to ensure a power of 80% with a 95% confidence interval between populations.

51. Khare, S. *et al.* An NLRP7-containing inflammasome mediates recognition of microbial lipopeptides in human macrophages. *Immunity* **36**, 464–476 (2012).
52. Shao, R. & Guo, X. Human microvascular endothelial cells immortalized with human telomerase catalytic protein: a model for the study of in vitro angiogenesis. *Biochem. Biophys. Res. Commun.* **321**, 788–794 (2004).
53. Bryan, N.B. *et al.* Differential splicing of the apoptosis-associated speck like protein containing a caspase recruitment domain (ASC) regulates inflammasomes. *J. Inflamm. (Lond.)* **7**, 23 (2010).
54. Bryan, N.B., Dorfleutner, A., Rojasasakul, Y. & Stehlik, C. Activation of inflammasomes requires intracellular redistribution of the apoptotic speck-like protein containing a caspase recruitment domain. *J. Immunol.* **182**, 3173–3182 (2009).
55. Fernandes-Alnemri, T. *et al.* The pyroptosome: a supramolecular assembly of ASC dimers mediating inflammatory cell death via caspase-1 activation. *Cell Death Differ.* **14**, 1590–1604 (2007).
56. Gross, S. *et al.* Bioluminescence imaging of myeloperoxidase activity *in vivo*. *Nat. Med.* **15**, 455–461 (2009).